Downregulation of cannabinoid receptor 1 from neuropeptide Y interneurons in the basal ganglia of patients with Huntington's disease and mouse models

Eric A. Horne[1], **Jonathan Coy**[1], **Katie Swinney**[1], **Susan Fung**[2], **Allison E. T. Cherry**[1], **William R. Marrs**[2], **Alipi V. Naydenov**[3], **Yi Hsing Lin**[1], **Xiaocui Sun**[1], **C. Dirk Keene**[4], **Eric Grouzmann**[5], **Paul Muchowski**[6,7], **Gillian P. Bates**[8], **Ken Mackie**[9], and **Nephi Stella**[1,10]

[1]Department of Pharmacology, University of Washington, 1959 N.E. Pacific St, BB-1538, HSC, Box 357280, Seattle, WA, 98195-7280, USA [2]Neurobiology and Behavior Graduate Program, University of Washington, Seattle, WA, USA [3]Medical Scientist Training Program, University of Washington, Seattle, WA, USA [4]Department of Pathology, University of Washington, Seattle, WA, USA [5]Division de Pharmacologie et Toxicologie Cliniques, Centre Hospitalier Universitaire Vaudois, Lausanne, Switzerland [6]Gladstone Institute of Neurological Disease, University of California, San Francisco, CA, USA [7]Departments of Biochemistry, Biophysics and Neurology, University of California, San Francisco, CA, USA [8]Division of Genetics & Molecular Medicine, Kings College, London, UK [9]Department of Psychological and Brain Sciences and Program in Neuroscience, Indiana University, Bloomington, IN, USA [10]Department of Psychiatry and Behavior, University of Washington, Seattle, WA, USA

Abstract

Cannabinoid receptor 1 (CB$_1$ receptor) controls several neuronal functions, including neurotransmitter release, synaptic plasticity, gene expression and neuronal viability. Downregulation of CB$_1$ expression in the basal ganglia of patients with Huntington's disease (HD) and animal models represents one of the earliest molecular events induced by mutant huntingtin (mHtt). This early disruption of neuronal CB$_1$ signaling is thought to contribute to HD symptoms and neurodegeneration. Here we determined whether CB$_1$ downregulation measured in patients with HD and mouse models was ubiquitous or restricted to specific striatal neuronal subpopulations. Using unbiased semi-quantitative immunohistochemistry, we confirmed previous studies showing that CB$_1$ expression is downregulated in medium spiny neurons of the indirect pathway, and found that CB$_1$ is also downregulated in neuropeptide Y (NPY)/neuronal nitric oxide synthase (nNOS)-expressing interneurons while remaining unchanged in parvalbumin- and calretinin-expressing interneurons. CB$_1$ downregulation in striatal NPY/nNOS-expressing interneurons occurs in R6/2 mice, Hdh$^{Q150/Q150}$ mice and the caudate nucleus of patients with HD. In R6/2 mice, CB$_1$ downregulation in NPY/nNOS-expressing interneurons correlates with diffuse expression of mHtt in the soma. This downregulation also occludes the ability of cannabinoid agonists to activate the pro-survival signaling molecule cAMP response element-binding protein in NPY/nNOS-expressing interneurons. Loss of CB$_1$ signaling in NPY/nNOS-expressing interneurons could contribute to the impairment of basal ganglia functions linked to HD.

Correspondence: Dr N. Stella, [1]University of Washington, as above. nstella@uw.edu.

Conflicts of interest
The authors report no conflict of interest.

Keywords

CB_1; CREB; neurodegeneration; NPY; R6/2

Introduction

Huntington's disease (HD) is an autosomal-dominant neurodegenerative disease caused by a poly-glutamine expansion of the protein huntingtin (Htt) resulting in the degeneration of striatal γ-aminobu tyricaid (GABA)ergic neurons, glutamatergic cortical neurons and hippocampal neurons (Group, 1993; Rosas *et al.*, 2003). Electrophysiological recordings from HD mouse models have demonstrated that striatal medium spiny neuron (MSN) excitability changes from hyperexcitable to hypoexcitable; a shift in the balance of glutamatergic and GABAergic signaling that augments as disease progresses (Cepeda *et al.*, 2003, 2004; Andre *et al.*, 2006; Cummings *et al.*, 2010). In addition, changes in the number of GABAergic interneurons expressing neuropeptide Y (NPY) or calretinin have been reported, and could contribute to the increased GABAergic tone in the striatum (Dawbarn *et al.*, 1985; Massouh *et al.*, 2008). Accordingly, patients with HD exhibit severe debilitating symptoms linked to the dysfunction of the basal ganglia (e.g. chorea and dystonia) that typically develop after the onset of cognitive impairments (Walker, 2007). Together these studies suggest that aberrant neuronal activity in the basal ganglia contributes to both the symptomatology and the progression of neurodegeneration associated with HD.

Presynaptic cannabinoid receptor 1 (CB_1 receptor) is expressed by both GABAergic and glutamatergic terminals (Herkenham *et al.*, 1991; Matyas *et al.*, 2006). Activation of these G-protein-coupled receptors inhibits presynaptic neurotransmitter release and regulates synaptic plasticity in the striatum (Gerdeman & Lovinger, 2001; Marsicano *et al.*, 2003; Kofalvi *et al.*, 2005; Kreitzer & Malenka, 2005). Thus, the downregulation of CB_1 receptors in HD mouse models could participate in the reported dysregulation of both GAB-Aergic neurotransmitter release and synaptic plasticity measured in these models (Cepeda *et al.*, 2003, 2004; Cummings *et al.*, 2010). Downregulation of total CB_1 receptor expression in the basal ganglia of adult patients with HD before symptom onset is well established, and has recently been detected in pre-symptomatic patients with HD by positron emission tomography (PET) imaging (Glass *et al.*, 1993, 2000; Dowie *et al.*, 2009; Van Laere *et al.*, 2010). *CNR1* mRNA and CB_1 receptor expression also decreases in the striatum of pre-symptomatic R6/1 and R6/2 HD mouse models (Mangiarini *et al.*, 1996; Denovan-Wright & Robertson, 2000). Recent evidence indicates that decreases in CB_1 receptor expression are likely due to mutant (m)Htt disrupting *CNR1* mRNA transcription, and that this deficit results in a functional loss of CB_1 receptor-mediated regulation of GABA release (Blazquez *et al.*, 2011; Chiodi *et al.*, 2011). Here we sought to determine whether CB_1 receptor loss is ubiquitous or restricted to specific striatal neuronal subpopulations.

Materials and methods

Antibodies and drugs

The following antibodies were used in this study: CB_1 (L15 pAb guinea pig 1 : 2000; Berghuis *et al.*, 2007); NPY [pAb rabbit 1 : 4000; Immunostar (Hudson, WI, USA) cat# 22940; mAb mouse 1 : 2000; Grouzmann *et al.*, 1992]; leucine-enkephalin [pAb rabbit 1 : 500; Millipore (Billerica, MA, USA) cat# AB5024]; Substance P (pAb rabbit 1 : 4000; Millipore cat# AB1566); parvalbumin (pAb rabbit 1 : 500; Immunostar cat# 24428); phosphorylated cAMP response element-binding protein (pCREB) [(p-Ser133) pAb rabbit 1 : 800; Cell Signaling Technology (Danvers, MA, USA) cat# 9198]; mHtt (mAb mouse clone mEM48 1 : 300; Millipore cat# MAB5374); calretinin (pAb rabbit 1 : 1000; Millipore

cat# AB5054); neuronal nitric oxide synthase (nNOS; CH_3-terminal, pAb 1 : 1000 rabbit; Immunostar cat# 24287); goat anti-rabbit Alexa-488, 555 and 647 [1 : 500; Invitrogen (Grand Island, NY, USA) cat# A11034, A21429, A21245]; goat anti-guinea pig Alexa-488 (1 : 500; Invitrogen cat# A11073); and goat anti-mouse Alexa-555 and 647 (1 : 500; Invitrogen cat# A21422, A21236). WIN 55,212-2 was purchased from Tocris Biosciences (Minneapolis, MN, USA).

R6/2 mice colony

Mice were housed in a specific pathogen-free facility in accordance with the National Institutes of Health, and the Institutional Animal Care and Use Committee at the University of Washington approved all experiments. Enrichment and *ad libitum* access to food and water were provided, and a 12-h light : dark cycle was maintained in the facility. R6/2 and wild-type littermates were given a wet food mash in addition to dry pellets beginning at 9 weeks old. Both female and male heterozygous and wild-type littermates were used in this study. The colony was maintained by breeding 6–8-week-old R6/2 males with two CBA/ C57Bl/6 females (Jackson Labs, Bar Harbor, ME, USA). The average CAG repeat length was 114.1 ± 0.3 ($n = 10$), and was determined by polymerase chain reaction (PCR) from tail snips by Laragen (Culver City, CA, USA). CB_1 receptor knockout colony was maintained by breading homozygote males with homozygote females from 6 to 8 weeks old (Marsicano *et al*, 2002). Experimenters were blind to the gender, genotype and age of all mice during tissue processing, image collection and digital image analysis.

Quantitative PCR (qPCR)

The cortex and striatum of R6/2 and littermate wild-type mice (4, 6, 8 and 12 weeks old) were dissected and rapidly stored in RNAlaterv® (Invitrogen). qPCR assays were performed using LightCycler 480 system [Roche Applied Science (Branchburg, NJ, USA)]. Probes for CB_1 receptor were from Roche Applied Science (Universal Probe Library: Set #47) and hypoxanthine phosphoribosyltransferase 1 (hprt1) from Applied Biosystems (Carlsbad, CA, USA) (VIC-tgcaaatacgaggagtcctgttgatgttgc-TAMRA). Primer sequences were: *CNR1* forward 5′-cgttcaaggagaacgaggac-3′ and reverse 5′-tgaagcactccatgtc-cataa-3′; *HPRT1* forward 5′-cctaagatgagcgcaagttgaa-3′ and reverse 5′-ccacaggactagaacacctgctaa-3′. Amplifications were run using a Stratagene Mx3000P QPCR system, and consisted of 30-min incubation at 45 °C, followed by 10 min at 95 °C, and 40 cycles of 1 min at 95 °C and 30 s at 60 °C.

Human tissue sections

The University of Washington Institutional Review Board approved this study. Appropriate measures for the protection of patient privacy were used. Paraffin-embedded human caudate-putamen tissue samples from HD and healthy patients were supplied by the University of Washington Alzheimer's Disease Research Center [ADRC; grant # P50 AG05136 (Seattle, WA, USA)]. Five patients with HD and age-matched non-HD patients were studied by semi-quantitative immunohistochemistry [sq-IHC; genotype, age, gender and Vonsattel grade were (Vonsattel *et al*, 1985): non-HD 74 female, non-HD 77 female, non-HD 78 male, non-HD 67 male, non-HD 52 male, HD 55 male (3), HD 20 female (3), HD 55 male (3), HD 43 male (2–3), HD 74 male (3)]. The patients with HD died from complications due to HD, while the non-HD patients died from non-CNS diseases and had normal brains.

Immunohistochemistry

Mice were killed and perfused with paraformaldehyde [PFA; 4% in phosphate-buffered saline (PBS)], post-fixed for 24 h, and their brains cryoprotected in 15% sucrose (24 h)

followed by 30% sucrose (48 h). Coronal sections that included the corticostriatal, globus pallidus or substantia nigra regions (30 μm) were prepared using a microtome, and then stored in PBS at 4 °C until processing. Sections from R6/2 mice and wild-type littermates were processed/ stained in parallel as follows – free-floating sections were rinsed 3× with PBS and incubated for 90 min at room temperature (RT) in PBS supplemented with donkey serum (5%) and Triton X-100 (1%). Primary antibody combinations were prepared as a master stock in PBS supplemented with donkey serum (2.5%) and Triton X-100 (0.5%), and applied to sections for 78 h at 4 °C with gentle agitation. Sections were then rinsed 8× with PBS supplemented with Tween-20 (0.05%, at RT) and incubated with secondary antibodies diluted in PBS supplemented with donkey serum (2.5%) and Triton X-100 (0.5%) for 1 h at RT with gentle agitation, followed by seven rinses with PBS and one rinse with deionized water. Sections were mounted onto slides and allowed to dry for ~ 18 h, after which cover slips were mounted with Vectashield and sealed with nail polish. For CREB phosphorylation studies, 12-week-old R6/2, CB_1 receptor knockout and wild-type littermates were injected with either vehicle (cremophore : ethanol : saline, 1 : 1 : 18) or WIN 55,212-2 (10 mg/kg, i.p.), returned to their home cage for 30 min, and then killed, perfused with 4% PFA, their brains dissected and stored in 10% neutral buffered formalin for paraffin embedding. Human and pCREB paraffin-embedded slices (5 and 4 μm, respectively) were deparaffinized with 3×5 min xylene washes followed by rehydrating washes in ethanol and antigen retrieval in citrate buffer (10 mM). Following addition of a hydrophobic barrier using an ImmunoPen™ (Millipore), sections were stained with the same protocol as the free-floating sections.

Microscopy

Dual-labeled images were collected on a Zeiss Axio Observer Z1 equipped with a Pan-Apochromatic 10×/0.3 numerical aperture (NA) air objective (to count somatic population) or a 63×/1.4 NA oil objective, ORCA-ER 1394 CCD camera [Hamamatsu (Hamamatsu City, Japan)] and AxioVision software [version 4.7.1, Zeiss (Jena, Germany)]. Illumination was set at 70% attenuation to limit photo bleaching and deconvolved using an Apotome (Optical Sectioning Average: medium; Noise: 3). Triple-labeled images were acquired using a Leica SP1 Confocal Laser Scanning microscope with a 40×/1.25 NA oil objective coupled to an argon laser (excites Alexa488), a DPSS laser (excites Alexa555) and a helium/neon laser (excites Alexa647) at the Keck Microscopy Facility of the University of Washington. Four scans were averaged using a 4× digital zoom with a medium scan rate and pinhole set at 102.9 μm. Sections that underwent parallel IHC staining were imaged using the same exposure settings. Five images of the dorsolateral striatum and layer V/VI of the sensorimotor cortex were taken per slice, and were processed for publication in parallel using Photoshop.

Semi-quantitative image analysis and statistics

Dual- and triple-labeled images were analysed and quantified using ImageJ (National Institutes of Health). Each channel was split into an individual image, and the mean intensity and standard deviation of each fluorophore in each image was measured. Background signal was removed by creating regions of interest (ROIs) for each fluorophore and setting the zero threshold value to the mean + standard deviation (Table 1). This threshold was used to analyse the 1/3 brightest pixels in the Poisson distribution of pixel intensity as the mean intensity is composed of a large majority of background intensities, as revealed by parallel staining of $CB_1R^{-/-}$ tissue. While this threshold excludes 'weakly' stained synapses, the remaining pixels that are analysed and quantified are comprised of positively stained pixels. ROIs 1–2 were used to collect the average intensity of each fluorophore, and selectively quantify axons and cell bodies that have positive staining. ROI 3 was created by making binary masks of each ROI and using the 'AND' function to create new ROIs that only contain regions with overlapping positive pixels from the original ROIs (Table 1). The

'Analysed Particles' function was then used to extrapolate the mean and standard deviation for each channel in each ROI. To quantify pCREB and mHtt levels, ROIs were hand-drawn around positively labeled somas as determined by thresholding the interneuron marker to a mean + standard deviation (interneuron soma ROI). Positive pCREB or mHtt in interneurons was determined by thresholding total pCREB or mHtt staining to a mean + standard deviation (pCREB/mHtt ROI) and combining it with the interneuron soma ROI using the 'AND' function in each image (pCREB/mHtt NPY ROI). The 'Analysed Particles' function was then used to extrapolate the mean and standard deviation for each channel in each ROI. Neurons whose percent area of pCREB staining to NPY soma staining was < 10% or > 50% [(# of pCREB NPY ROI-positive pixels/# of NPY soma ROI-positive pixels) *100%] were excluded, so only interneurons that contained pCREB translocated to the nucleus were quantified [based on the average percent area of positive pCREB pixels in NPY interneurons with visible nuclei treated with either vehicle (24.9 ± 18.1%) or WIN 55,212–2 (42.2 ± 1.8%); these values specifically reported as standard deviations]. Mask statistics were then used to calculate the mean and standard deviation for each channel in each mask. All values were imported into Excel [Microsoft® Office 2008 Version 12.2.7 (Redmond, WA, USA)], and means were normalized to wild-type expression for comparison. All values are expressed as mean ± standard error of the mean.

Statistical analysis

Statistical analysis and graphs were generated using GRAPHPAD PRISM (version 4; San Diego, CA, USA). Comparisons of mean intensities between genotype at specific ages were analysed by Student's *t*-test. Comparisons between interneuron subtypes within R6/2 mice or pCREB levels between genotypes were analysed by one-way ANOVA with a Tukey's *post hoc* analysis, while a two-way ANOVA was used to analyse qPRC data. Data were considered significant if $P < 0.05$.

Results

CB$_1$ receptor expression is decreased in R6/2 mouse striatum

It is known that CB$_1$ receptor expression is decreased in the basal ganglia of various HD mouse models (Fernandez-Ruiz, 2009). In agreement with several studies, we found that *CNR1* mRNA expression decreased in R6/2 mice as a function of disease progression (Denovan-Wright & Robertson, 2000; Luthi-Carter *et al*, 2000; McCaw *et al*, 2004; Blazquez *et al*, 2011; Chiodi *et al*, 2011). Specifically, using qPCR we found that *CNR1* mRNA is decreased by 25.6 ± 5.6% in the striatum of R6/2 at 4 weeks old, and that this downregulation reached its lowest level at 6 weeks old (57.7 ± 4.8% compared with wild-type: df = 1, F = 72.495, $P < 0.05$; Fig. 1A). *CNR1* mRNA in the cortex of R6/2 mice decreased by 20.3 ± 1.6% at 4 weeks old, and by 43.6 ± 2.5% at 12 weeks old (R6/2 compared with wild-type: df = 1, F = 18.839, $P < 0.05$; Fig. 1A).

To determine if the expression of CB$_1$ receptor protein was concomitantly decreased to *CNR1* mRNA, a sq-IHC analysis of corticostriatal slices from R6/2 mice was performed. Control experiments confirmed that CB$_1$ receptor protein expression displays a stereotypical axonal pattering in the striatum of wild-type mice [(Uchigashima *et al*, 2007; Fig. 1B], and that this immunostaining is absent in CB$_1^{-/-}$ mice (Fig. 1C, insert). Remarkably, CB$_1$ receptor protein staining in R6/2 striatum appeared more punctate (Fig. 1C). When quantifying CB$_1$ receptor expression by sq-IHC and defining ROIs for CB$_1$ receptor-positive axons (see Materials and methods for details; Fig. 2A and B), we found that CB$_1$ receptor loss in the striatum of R6/2 mice was delayed and less pronounced compared with the loss of *CNR1* mRNA, reaching a 16.2 ± 3.9% decrease in CB$_1$ receptor protein at 12 weeks old as compared with wild-type littermates (CB$_1$ receptor expression normalized to age-matched

wild-type littermates: 4 weeks, $P = 0.77$; 8 weeks, $P = 0.52$; 12 weeks, $P < 0.001$; Fig. 1D). CB_1 receptor protein staining in layers V/VI of the sensorimotor cortex remained unchanged throughout the disease progression (CB_1 receptor expression normalized to age-matched wild-type littermates: 4 weeks, $P = 0.28$; 8 weeks, $P = 0.11$; 12 weeks, $P = 0.60$; Fig. 1E).

Approximately 95% of the striatal neurons are GABAergic MSNs, which project to the substantia nigra reticulata in the direct pathway and the globus pallidus in the indirect pathway. Because *CNR1* mRNA in R6/2 striatum is significantly decreased and the majority of CB_1 receptors traffic to presynaptic axon terminals following translation (Matyas *et al.*, 2006), we measured whether CB_1 receptor expression in the substantia nigra reticulata and the globus pallidus of R6/2 mice was also decreased. We found that at 12 weeks old, CB_1 receptor protein levels in R6/2 mice were decreased in the globus pallidus by $26.4 \pm 10.9\%$ compared with wild-type, while remaining unchanged in the substantia nigra reticulata [CB_1 receptor expression normalized to age-matched wild-type littermates (globus pallidus): 4 weeks, $P < 0.01$; 8 weeks, $P < 0.001$; 12 weeks, $P < 0.05$; (substantia nigra reticulate): 4 weeks, $P = 0.22$; 8 weeks, $P = 0.55$; 12 weeks, $P = 0.48$; Fig. 1F]. Interestingly, the combined fold decrease in CB_1 receptor protein measured in both the globus pallidus and the striatum at 12 weeks ($13.9 + 26.4\% = 40.3\%$) is within the range of the decrease in *CNR1* mRNA measured in the striatum (46.3%) at this age. This result suggests that the loss of *CNR1* mRNA in the striatum is not a ubiquitous decrease in *CNR1* mRNA among all neuronal subpopulations, but is rather a selective decrease in specific neuronal subpopulations. Together, these results suggest that CB_1 receptor downregulation occurs in MSNs belonging to the indirect pathway and in a yet unidentified neuronal subpopulation within the striatum.

Downregulation of CB_1 receptor protein in the striatum is selective to both NPY/nNOS+ interneurons and indirect pathway MSNs

Studies reporting the electrophysiological measurements in the striatum of R6/2 mice demonstrate that overall GABAergic transmission is increased at disease end-stage (12 weeks old), and CB_1 receptor-mediated inhibition of GABA release is lost in 12-week-old R6/2 mice (Cepeda *et al.*, 2004; Chiodi *et al.*, 2011). Here we tested if CB_1 receptor expression is changed in all subpopulations of striatal GABAergic neurons known to express CB_1 receptors: MSNs, parvalbumin interneurons, calretinin interneurons and NPY interneurons (Fusco *et al.*, 2004; Narushima *et al.*, 2006; Uchigashima *et al*, 2007). Cholinergic interneurons in the striatum of wild-type mice lack CB_1 receptors and thus were not analysed (Hohmann & Herkenham, 2000). To quantify CB_1 receptor expression in these neuronal subpopulations, we performed sq-IHC of corticostriatal slices from R6/2 mice and their wild-type littermates (double-labeled with antibodies directed against CB_1 receptors and specific neuronal markers). For MSN, we stained for the direct (substance P) and indirect (leucine-enkephalin) pathways, thus labeling the collaterals that project within the striatum. To identify interneurons, we co-labeled for parvalbumin, calretinin or NPY (Fig. 2A and B). In agreement with the decrease of the CB_1 receptor found in the globus pallidus, a $14.2 \pm 6.2\%$ decrease in indirect pathway MSN axon collaterals was observed (CB_1 receptor in leucine-enkephalin normalized to wild-type littermate: $P = 0.025$; Fig. 2C). CB_1 receptor was also decreased by $20.3 \pm 3.5\%$ at NPY interneurons, while remaining unchanged at parvalbumin and calretinin interneurons, as well as in the axonal collaterals of direct pathway MSN within the striatum of R6/2 mice [CB_1 receptor in neuronal subtypes normalized to wild-type littermate (NPY): $P < 0.001$; (substance P): $P = 0.54$; (parvalbumin): $P = 0.68$; (calretinin): $P = 0.87$; Fig. 2C].

A recent study has demonstrated that NPY interneurons in the striatum consist of two distinct populations of GABAergic interneurons (Ibanez-Sandoval *et al*, 2011). Approximately 90% of NPY interneurons are low-threshold spiking (LTS) interneurons that

express NOS and somatostatin (NPY/nNOS+); the remaining 10% of NPY interneurons lack somatostatin and NOS (NPY/nNOS—) and display a distinct electrophysiological profile, suggesting they perform a unique role in the striatal microcircuitry (Ibanez-Sandoval *et al*, 2011). To test whether CB_1 receptor expression was decreased in these subclasses of NPY interneurons in 12-week-old R6/2 mice, corticostriatal slices were triple-labeled for CB_1 receptor, NPY and nNOS. sq-IHC analysis on NPY/nNOS— interneurons showed no significant decrease in CB_1 receptor expression (CB_1 receptor normalized to wild-type littermates: $P = 0.21$; Fig 2D). These results indicate that the decrease of CB_1 receptors in NPY interneurons is selective to the main NPY interneuron subtype, the LTS NPY/nNOS+ interneurons.

Downregulation of CB_1 protein in NPY interneurons of $Hdh^{Q150/Q150}$ knock-in mice and human patients with HD

Decreased striatal *CNR1* mRNA also occurs in the full-length HD mouse model (Lin *et al*, 2001; Woodman *et al*, 2007). Here we sought to determine if the expression of CB_1 receptor protein was also decreased in NPY interneurons in two full-length HD models ($Hdh^{Q150/Q150}$ and BACHD; Woodman *et al*., 2007; Gray *et al*., 2008). Coronal corticostriatal sections of $Hdh^{Q150/Q150}$ mice (16–17 months old) and BACHD (9 months old) were co-labeled for CB_1 receptor and NPY. Similar to what we detected in R6/2 mice, CB_1 receptor expression in the striatum of $Hdh^{Q150/Q150}$ mice was decreased by $15.8 \pm 6.5\%$ in the striatum as a whole (CB_1 receptor in $Hdh^{Q150/Q150}$ normalized to wild-type littermates: $P = 0.019$; data not shown) and by $13.5 \pm 6.5\%$ at NPY interneurons (CB_1 receptor in NPY interneurons of $Hdh^{Q150/Q150}$-normalized wild-type littermates: $P = 0.042$; Fig. 3A). In contrast, CB_1 receptor expression remained unchanged both in the striatum as a whole (CB_1 receptor in BACHD normalized to wild-type littermates: $P = 0.12$; data not shown) and at NPY interneurons in BACHD mice compared with their wild-type littermates (CB_1 receptor in NPY interneurons of BACHD-normalized wild-type littermates: $P = 0.23$; Fig 3A). These results suggest that not all HD mice models reproduce the downregulation of CB_1 receptor known to occur in patients with HD.

A recent PET study demonstrated that downregulation of CB_1 receptor in the striatum of human presymptomatic patients with HD can be detected (Van Laere *et al*., 2010), extending autoradiography studies that had detected a global loss of CB_1 receptor in the caudate and putamen of patients with HD as early as grade 0 (neuropathological grading scale criteria of Vonsattel and colleagues; Vonsattel *et al*., 1985; Glass *et al*., 2000). This loss has been attributed to the loss of CB_1 receptor from MSN, first from indirect pathway MSNs in early stages of the disease and then spreading to direct pathway MSNs in later stages (Richfield & Herkenham, 1994; Glass *et al*., 2000). To determine if CB_1 receptors at NPY interneurons are also downregulated in human patients with HD, sq-IHC was performed on the caudate and putamen tissue sections from patients with HD. We found a $15.2 \pm 3.6\%$ decrease of CB_1 receptors in NPY interneurons located in the caudate nucleus of patients with HD compared with non-HD patients [CB_1 receptor in NPY interneuron of patients with HD normalized to non-HD patients (caudate): $P < 0.001$; (putamen): $P = 0.8$; Fig. 3B]. These results suggest that the decrease of CB_1 receptors at NPY neurons is a common phenomenon occurring in both human patients with HD and HD mouse models.

NPY interneurons display diffuse mHtt load in R6/2 mice

mHtt forms aggregates within the nucleus and micro-aggregates within the cytoplasma of neuropila that have been implicated in disrupting specific cellular mechanisms, including gene transcription and axonal protein transport, both of which control CB_1 receptor expression and distribution within neurons (Li *et al*, 1999; Lee *et al*, 2004). To investigate if mHtt formed nuclear aggregates in NPY interneurons, corticostriatal slices were double-

labeled for mHtt and the three GABAergic interneuron subtypes. We found that large mHtt aggregates were prominently located in parvalbumin interneurons in the striatum of 12-week-old R6/2 (Fig. 4A). While it is thought that mHtt aggregates in a cell-autonomous manner, calretinin interneurons express very low levels of mHtt and do not display the large aggregates observed in parvalbumin interneurons (Fig. 4B). Some NPY interneurons displayed large aggregates similar to parvalbumin interneurons, but the majority of mHtt expression within NPY interneurons appeared as diffuse staining suggesting the presence of micro-aggregates (Fig. 4C). Interestingly, small mHtt aggregates were observed in some NPY neurites (Fig. 4C1). Semi-quantitative analysis confirmed that parvalbumin interneurons contain 130% higher levels of mHtt compared with calretinin interneurons and 105% higher levels compared with NPY interneurons [mHtt in interneuron subtypes normalized to mHtt in calretinin interneurons: $F = 15.73$, $P < 0.001$ (parvalbumin vs. calretinin, and parvalbumin vs. NPY); Fig. 4D]. These results indicate that the presence of micro-aggregate mHtt correlates with the decrease in CB_1 receptor expression in NPY interneurons.

A recent study suggested that monomeric or micro-aggregates represent the toxic form of mHtt that could participate in neurodegeneration (Miller *et al*, 2011). To determine if the number of NPY cells is reduced in R6/2 mice, NPY-positive somas were outlined and counted in both R6/2 mice and human patients with HD. We found that the overall number of NPY interneurons within the striatum of R6/2 mice was not lost (11.7 ± 5.8 NPY interneurons/ 500 000 μm^2 in wild-type vs. 10.1 ± 5.4 NPY interneurons/ 500 000 μm^2 in R6/2; $P = 0.07$; Fig. 5A). However, closer inspection of the two subtypes of NPY interneurons revealed that the number of NPY/nNOS– interneurons is significantly reduced in the dorsolateral striatum of 12-weeks-old R6/2 mice (1.6 ± 0.3 NPY interneurons/500 000 um^2 in wild-type vs. 0.4 ± 0.1 NPY interneurons/500 000 μm^2 R6/2; $P = 0.012$; data not shown). In human patients with HD, NPY interneurons were spared in the caudate (where CB_1 receptor levels are decreased at NPY interneurons; 1.7 ± 0.29 NPY interneurons/500 000 μm^2 in patients with HD vs. 1.6 ± 0.20 NPY interneurons/500 000 μm^2 in non-HD patients), but were significantly higher in the putamen [where CB_1 receptors are spared; 3.5 ± 0.40 NPY interneurons/500 000 μm^2 in patients with HD vs. 1.8 ± 0.25 NPY interneurons/500 000 μm^2 in non-HD patients; $F = 9.357$, $P < 0.001$ (non-HD putamen vs. HD putamen, HD putamen vs. HD caudate, HD putamen vs. non-HD caudate); Fig. 5B]. These results confirm previous studies that also found an increase in the number of NPY interneurons in the caudate and putamen of patients with HD (Dawbarn *et al.*, 1985).

Functional loss of CREB signaling downstream of CB_1 receptors activation in striatal NPY interneurons in R6/2 mice

Activation of CREB through phosphorylation of serine 133 (pCREB) regulates cell survival pathways, and defects in this signaling pathway are thought to contribute to the neurodegeneration of MSN in the dorsolateral striatum (Mantamadiotis *et al.*, 2002). Acute activation of CB_1 receptors increases pCREB levels in the brain and, accordingly, CB_1 receptor downregulation could lead to a decrease in pCREB levels at specific neuronal subtypes (Rubino *et al.*, 2006; Isokawa, 2009). To test if decreased CB_1 receptor expression in R6/ 2 mice affected CREB signaling, we treated 12-week-old R6/2 mice and their wild-type littermates with the CB_1 receptor agonist WIN 55,212–2 and measured changes in pCREB levels in NPY interneurons located within the dorsolateral striatum by sq-IHC. While CB_1 receptor activation in wild-type mice caused a significant $12.4 \pm 2.5\%$ increase in the amount of pCREB in striatal NPY interneurons of wild-type mice [pCREB in NPY of R6/2 normalized to pCREB in NPY of wild-type littermate: F = 5.677, $P < 0.001$ (wild-type WIN 55,212–2 vs. wild-type vehicle and knockout vehicle), $P < 0.05$ (wild-type WIN 55,212-2 vs. R6/2 vehicle and R6/2 WIN 55,212–2); Fig. 6A, B and E], this treatment did

not increase pCREB in NPY interneurons of R6/2 or CB_1 knockout mice (F = 5.677, $P >$ 0.05; Fig. 6C – E). These results suggest that CB_1 receptor downregulation results in a functional loss of cannabinoid-dependent pCREB signaling in striatal NPY interneurons of R6/2 mice.

Discussion

By using sq-IHC as an unbiased approach, we confirmed that CB_1 receptor expression is decreased in the indirect pathway MSN early in the disease of R6/2 mice, and discovered that it is also decreased in NPY/nNOS+ interneurons but later in the disease progression. We validated this result in a slower progressing (full-length) mHtt knock-in model of HD ($Hdh^{Q150/Q150}$), as well as in the caudate nucleus of patients with HD. In R6/2 mice, decreased CB_1 receptor expression in NPY/nNOS+ interneurons correlated with diffuse mHtt expression and occluded the cannabinoid-stimulated activation of pCREB signaling in these cells. Due to the postulated role played by NPY/nNOS+ interneurons in regulating basal ganglia function, this selective loss of CB_1 receptor signaling in this class of interneuron could contribute to disrupting basal ganglia function in HD.

Glass *et al.* first reported the loss of CB_1 receptor from the globus pallidus in pre-symptomatic patients with HD (Glass *et al.*, 2000), a result that propelled many laboratories to study if and how this early molecular dysfunction occurs in various HD cellular and *in vivo* models. Our study shows that in R6/2 mice, early in the disease, CB_1 receptor expression is decreased in the globus pallidus, while it is not affected in the striatum (where these terminals originate). Accordingly, striatal *CNR1* mRNA, the majority of which is likely from MSNs, also decreases early in disease, providing a correlation between the early loss in both *CNR1* mRNA in the neuronal soma and the loss of CB_1 protein in the presynaptic terminals of these neurons. Our results suggest that the majority of *CNR1* mRNA loss measured in the striatum belongs to MSNs of the indirect pathway. This result agrees with MSNs comprising >95% of the neurons of the striatum, and suggests that loss of CB_1 protein in indirect pathway MSN could contribute to the enhanced susceptibility of these projections to neuronal dysfunction during HD pathogenesis. Our results obtained in R6/2 mice extend earlier studies performed on post mortem patients with HD demonstrating that CB_1 receptor binding is first decreased in the globus pallidus of presymptomatic patients with HD followed by loss in the striatum and the substantia nigra reticulata as the disease progresses (Glass *et al.*, 1993, 2000).

Decreases in CB_1 protein expression in specific neuronal subtypes could be due to multiple mechanisms. Evidence indicates that mHtt directly interferes with the molecular machinery controlling *CNR1* gene transcription, decreasing *CNR1* mRNA expression in various HD models (McCaw *et al.*, 2004; Blazquez *et al.*, 2011). Because the decrease in CB_1 receptor expression is specific to certain neuronal subtypes, it is unlikely that reduction in *CNR1* transcription represents the sole molecular mechanism responsible for decreasing CB_1 receptor expression in cells. mHtt is also known to form micro-aggregates in axons of MSN that inhibit anterograde axonal transport of molecules to axonal boutons (DiFiglia *et al.*, 1997; Gunawardena *et al.*, 2003; Lee *et al.*, 2004; Her & Goldstein, 2008). One hypothesis is that mHtt-mediated disruption of anterograde axonal transport could participate in the cell-specific decrease of CB_1 receptor expression at axonal boutons, possibly resulting in the punctate staining of CB_1 receptor observed in the striatum of R6/2 mice. The correlation between the diffuse mHtt staining in the nucleus associated with mHtt aggregates in the neuropila of NPY interneurons and the cell-specific decrease of CB_1 receptor at these interneurons supports a role for micro-aggregates in both of these mechanisms. Accordingly, there is a correlation between the presence of large aggregate loads in parvalbumin interneurons and the stability of CB_1 receptors expression in these neurons. These results

agree with *in vitro* studies showing that larger mHtt aggregates might represent a protective mechanism (Arrasate *et al.*, 2004). Interestingly, the BACHD mouse model accumulates very few mHtt aggregates and lacks nuclear localization of mHtt in the striatum, while still displaying a large aggregate load in the cortex (Gray *et al.*, 2008). Thus, the lack of CB_1 receptor loss in the striatum of BACHD mice could reflect a lack of transcriptional and anterograde transport dysregulation in the striatum of this mouse model. Here our results suggest that in addition to transcriptional dysregulation of CNR1, the trafficking of CB_1 protein down axons of MSNs projecting to the globus pallidus might be impaired by mHtt aggregates.

Decreased expression and functionality of CB_1 receptor at NPY/ nNOS+ interneurons could have multiple functional implications on striatal output. NPY interneurons comprise about 1% of neurons within the striatum and can be divided into two distinct subtypes that display unique electrophysiological properties. Interestingly, the loss of CB_1 receptor is specific to the prominent NPY/nNOS+ subtype, which are LTS GABAergic interneurons that establish synaptic connections with the distal dendrites of both MSN and cholinergic interneurons (Kreitzer, 2009; Tepper *et al.*, 2010). Paired recordings of NPY/nNOS+ interneurons onto MSNs from healthy tissue revealed that these synapses induce weak inhibitory postsynaptic currents (IPSCs; Gittis *et al.*, 2010). Accordingly, CB_1 receptor downregulation at GABAergic synapses of NPY/nNOS+ interneurons would enhance GABA release onto MSN and intensify these IPSCs, a response measured in MSNs from both R6/2 and Hdh$^{Q150/ Q150}$ mice (Cepeda *et al.*, 2004; Cummings *et al.*, 2010). In support of this idea, a study by Dehorter *et al.* showed that under conditions where dopamine is depleted in the striatum – a condition observed in both Parkinson's disease and HD – LTS NPY interneurons switch from eliciting a weak GABAergic signal to large oscillating IPSCs onto MSNs (Johnson *et al.*, 2006; Dehorter *et al.*, 2009; Callahan & Abercrombie, 2011). Because the production and release of endocannabinoids are controlled by dopamine receptor activation (Giuffrida *et al.*, 1999; Kreitzer & Malenka, 2005), reduction of both dopamine-mediated endocannabinoid production and downregulation of CB_1 receptor signaling in these interneurons could impair the corticostriatal-MSN-NPY/nNOS+ interneuron microcircuits, and ultimately the output function of these neuronal connections forming the basal ganglia.

To determine if decreased CB_1 receptor expression affected NPY/ nNOS+ interneuron physiology, we used sq-IHC to measure CB_1 receptor agonist-induced increases in pCREB levels in these cells. We chose this readout because activation of CREB by phosphorylation controls both synaptic plasticity and enhanced cell survival, and loss of CREB binding protein activity downstream of pCREB has been implicated in HD (Silva *et al.*, 1998; Finkbeiner, 2000). CB_1 receptor activation increases pCREB levels in both mouse brain (neuronal network model) and cells in culture (cell-autonomous model; Rubino *et al.*, 2006; Isokawa, 2009; Hudson *et al.*, 2010). To date we still do not understand the molecular and cellular details of the pCREB response induced by cannabinoids. One possibility is that activation of CB_1 receptors expressed by neurons connecting with NPY/nNOS+ interneurons regulates the amount of pCREB in these cells by producing endocannabinoids. Specifically, activation of synaptic glutamatergic *N*-methyl-ᴅ-aspartic acid (NMDA) receptors increases CREB phosphorylation (Hardingham *et al.*, 2002; Mantamadiotis *et al.*, 2002), while activation of extrasynaptic NMDA receptor subunit 2B (NR2B)-containing NMDA receptors, due to excessive glutamate release, opposes pCREB increases. Activation of NMDA receptors also increases endocannabinoid production from neurons (Stella & Piomelli, 2001). CB_1 receptor activation decreases the level of glutamate release from presynaptic terminals, thus decreased CB_1 receptor activation could lead to excessive glutamate release leading to the activation of extrasynaptic NR2B–containing NMDA, which have been implicated in HD progression (Hardingham *et al.*, 2002; Heng *et al.*, 2009;

Okamoto *et al.*, 2009; Milnerwood *et al.*, 2010). With regard to the involvement of a cell-autonomous mechanism, CB_1 receptors expressed on the soma and dendrites of neurons are thought to activate neuroprotective pathways, including pERK, a signaling pathway upstream of pCREB, which is critical for cell survival in neurons undergoing excitotoxic challenges (Bouaboula *et al.*, 1995; Derkinderen *et al.*, 2003; Marsicano *et al.*, 2003). Experiments in heterologous cell models show that CB_1 receptor activation increases pCREB levels, demonstrating that CB_1 receptors can directly couple to this signaling pathway (Graham *et al.*, 2006; Hudson *et al.*, 2010). Because NPY/nNOS+ interneurons receive sparse glutamatergic innervations (Gittis *et al.*, 2010), we propose that the CB_1 receptor activation leads to increases in pCREB in NPY/nNOS+ interneurons through a cell-autonomous mechanism. Together, these results suggest that CB_1 receptor downregulation leads to a functional loss of cannabinoid-mediated control of pCREB signaling in striatal NPY/nNOS+ interneurons of R6/2 mice.

In conclusion, our study identified an additional neuronal subtype with decreased CB_1 receptor expression within the striatum of HD mice models and patients. Because of the known function of these G-protein-coupled receptors in controlling neuron responses and participation in neuronal networks (Palop *et al.*, 2006; Miller & Bezprozvanny, 2010), as well as the function of NPY/nNOS+ interneurons in regulating the output function of the basal ganglia, our study suggests that loss of CB_1 receptor function in NPY interneurons might be involved in the symptoms and pathogenesis associated with HD.

Acknowledgments

Abbreviations

CB_1 receptor	cannabinoid receptor 1
CREB	cAMP response element-binding protein
GABA	γ-aminobutyric acid
HD	Huntington's disease
Htt	huntingtin protein
IPSC	inhibitory postsynaptic current
LTS	low-threshold spiking
mHtt	mutant huntingtin
MSN	medium spiny neuron
NA	numerical aperture
NMDA	*N*-methyl-D-aspartic acid
nNOS	neuronal nitric oxide synthase
NPY	neuropeptide Y
NR2B	NMDA receptor subunit 2B
PBS	phosphate-buffered saline
PCR	polymerase chain reaction

|	
pCREB	phosphorylated CREB
PET	positron emission tomography
PFA	paraformaldehyde
qPCR	quantitative polymerase chain reaction
ROI	region of interest
RT	room temperature
sq-IHC	semi-quantitative immunohistochemistry

References

Andre VM, Cepeda C, Venegas A, Gomez Y, Levine MS. Altered cortical glutamate receptor function in the R6/2 model of Huntington's disease. J. Neurophysiol. 2006; 95:2108–2119. [PubMed: 16381805]

Arrasate M, Mitra S, Schweitzer ES, Segal MR, Finkbeiner S. Inclusion body formation reduces levels of mutant huntingtin and the risk of neuronal death. Nature. 2004; 431:805–810. [PubMed: 15483602]

Berghuis P, Rajnicek AM, Morozov YM, Ross RA, Mulder J, Urban GM, Monory K, Marsicano G, Matteoli M, Canty A, Irving AJ, Katona I, Yanagawa Y, Rakic P, Lutz B, Mackie K, Hark-any T. Hardwiring the brain: endocannabinoids shape neuronal connectivity. Science. 2007; 316:1212–1216. [PubMed: 17525344]

Blazquez C, Chiarlone A, Sagredo O, Aguado T, Pazos R, Resel E, Palazuelos J, Julien B, Salazar M, Borner C, Benito C, Carrasco C, Diez-Zaera M, Paoletti P, Guzman M. Loss of striatal CB1 cannabinoid receptors is a key pathogenic factor in Huntington's disease. Brain. 2011; 134:119–136. [PubMed: 20929960]

Bouaboula M, Poinot-Chazel C, Bourrie B, Canat X, Calandra B, Ri-naldi-Carmona M, Le Fur G, Casellas P. Activation of mitogen-activated protein kinases by stimulation of the central cannabinoid receptor CB1. Biochem. J. 1995; 312(Pt 2):637–641. [PubMed: 8526880]

Callahan JW, Abercrombie ED. *In vivo* dopamine efflux is decreased in striatum of both fragment (R6/2) and full-length (YAC128) transgenic mouse models of Huntington's disease. Front. Syst. Neurosci. 2011; 5:61. [PubMed: 21811446]

Cepeda C, Hurst RS, Calvert CR, Hernandez-Echeagaray E, Nguyen OK, Jocoy E, Christian LJ, Ariano MA, Levine MS. Transient and progressive electrophysiological alterations in the corticostriatal pathway in a mouse model of Huntington's disease. J. Neurosci. 2003; 23:961–969. [PubMed: 12574425]

Cepeda C, Starling AJ, Wu N, Nguyen OK, Uzgil B, Soda T, Andre VM, Ariano MA, Levine MS. Increased GABAergic function in mouse models of Huntington's disease: reversal by BDNF. J. Neurosci. Res. 2004; 78:855–867. [PubMed: 15505789]

Chiodi V, Uchigashima M, Beggiato S, Ferrante A, Armida M, Mar-tire A, Potenza RL, Ferraro L, Tanganelli S, Watanabe M, Domenici MR, Popoli P. Unbalance of CB1 receptors expressed in GABAergic and glutamatergic neurons in a transgenic mouse model of Huntington's disease. Neurobiol. Dis. 2011; 45:983–991. [PubMed: 22207189]

Cummings DM, Cepeda C, Levine MS. Alterations in striatal synaptic transmission are consistent across genetic mouse models of Huntington's disease. ASN Neuro. 2010; 2:e00036. [PubMed: 20585470]

Dawbarn D, De Quidt ME, Emson PC. Survival of basal ganglia neuropeptide Y-somatostatin neurones in Huntington's disease. Brain Res. 1985; 340:251–260. [PubMed: 2862959]

Dehorter N, Guigoni C, Lopez C, Hirsch J, Eusebio A, Ben-Ari Y, Hammond C. Dopamine-deprived striatal GABAergic interneurons burst and generate repetitive gigantic IPSCs in medium spiny neurons. J. Neurosci. 2009; 29:7776–7787. [PubMed: 19535589]

Denovan-Wright EM, Robertson HA. Cannabinoid receptor messenger RNA levels decrease in a subset of neurons of the lateral striatum, cortex and hippocampus of transgenic Huntington's disease mice. Neuro-science. 2000; 98:705–713.

Derkinderen P, Valjent E, Toutant M, Corvol JC, Enslen H, Ledent C, Trzaskos J, Caboche J, Girault JA. Regulation of extracellular signal-regulated kinase by cannabinoids in hippocampus. J. Neurosci. 2003; 23:2371–2382. [PubMed: 12657697]

DiFiglia M, Sapp E, Chase KO, Davies SW, Bates GP, Vonsattel JP, Aronin N. Aggregation of huntingtin in neuronal intranuclear inclusions and dystrophic neurites in brain. Science. 1997; 277:1990–1993. [PubMed: 9302293]

Dowie MJ, Bradshaw HB, Howard ML, Nicholson LF, Faull RL, Hannan AJ, Glass M. Altered CB1 receptor and endocannabinoid levels precede motor symptom onset in a transgenic mouse model of Huntington's disease. Neuroscience. 2009; 163:456–465. [PubMed: 19524019]

Fernandez-Ruiz J. The endocannabinoid system as a target for the treatment of motor dysfunction. Br. J. Pharmacol. 2009; 156:1029–1040. [PubMed: 19220290]

Finkbeiner S. CREB couples neurotrophin signals to survival messages. Neuron. 2000; 25:11–14. [PubMed: 10707967]

Fusco FR, Martorana A, Giampà C, De March Z, Farini D, D'Angelo V, Sancesario G, Bernardi G. Immunolocalization of CB1 receptor in rat striatal neurons: a confocal microscopy study. Synapse. 2004; 53:159–167. [PubMed: 15236348]

Gerdeman G, Lovinger DM. CB1 cannabinoid receptor inhibits synaptic release of glutamate in rat dorsolateral striatum. J. Neurophysiol. 2001; 85:468–471. [PubMed: 11152748]

Gittis AH, Nelson AB, Thwin MT, Palop JJ, Kreitzer AC. Distinct roles of GABAergic interneurons in the regulation of striatal output pathways. J. Neurosci. 2010; 30:2223–2234. [PubMed: 20147549]

Giuffrida A, Parsons LH, Kerr TM, Rodriguez de Fonseca F, Navarro M, Piomelli D. Dopamine activation of endogenous cannabinoid signaling in dorsal striatum. Nat. Neurosci. 1999; 2:358–363. [PubMed: 10204543]

Glass M, Faull RL, Dragunow M. Loss of cannabinoid receptors in the substantia nigra in Huntington's disease. Neuroscience. 1993; 56:523–527. [PubMed: 8255419]

Glass M, Dragunow M, Faull RL. The pattern of neurodegeneration in Huntington's disease: a comparative study of cannabinoid, dopamine, adenosine and GABA(A) receptor alterations in the human basal ganglia in Huntington's disease. Neuroscience. 2000; 97:505–519. [PubMed: 10828533]

Graham ES, Ball N, Scotter EL, Narayan P, Dragunow M, Glass M. Induction of Krox-24 by endogenous cannabinoid type 1 receptors in Neuro2A cells is mediated by the MEK-ERK MAPK pathway and is suppressed by the phosphatidylinositol 3-kinase pathway. J. Biol. Chem. 2006; 281:29085–29095. [PubMed: 16864584]

Gray M, Shirasaki DI, Cepeda C, Andre VM, Wilburn B, Lu XH, Tao J, Yamazaki I, Li SH, Sun YE, Li XJ, Levine MS, Yang XW. Full-length human mutant huntingtin with a stable polyglutamine repeat can elicit progressive and selective neuropathogenesis in BACHD mice. J. Neurosci. 2008; 28:6182–6195. [PubMed: 18550760]

Group Hs.D.C.R. A novel gene containing a trinucleotide repeat that is expanded and unstable on Huntington's disease chromosomes. The Huntington's Disease Collaborative Research Group. Cell. 1993; 72:971–983. [PubMed: 8458085]

Grouzmann E, Comoy E, Walker P, Burnier M, Bohuon C, Waeber B, Brunner H. Production and characterization of four anti-neuropeptide Y monoclonal antibodies. Hybridoma. 1992; 11:409–424. [PubMed: 1383123]

Gunawardena S, Her LS, Brusch RG, Laymon RA, Niesman IR, Gordesky-Gold B, Sintasath L, Bonini NM, Goldstein LS. Disruption of axonal transport by loss of huntingtin or expression of pathogenic polyQ proteins in Drosophila. Neuron. 2003; 40:25–40. [PubMed: 14527431]

Hardingham GE, Fukunaga Y, Bading H. Extrasynaptic NMDARs oppose synaptic NMDARs by triggering CREB shut-off and cell death pathways. Nat. Neurosci. 2002; 5:405–414. [PubMed: 11953750]

Heng MY, Detloff PJ, Wang PL, Tsien JZ, Albin RL. *In vivo* evidence for NMDA receptor-mediated excitotoxicity in a murine genetic model of Huntington disease. J. Neurosci. 2009; 29:3200–3205. [PubMed: 19279257]

Her LS, Goldstein LS. Enhanced sensitivity of striatal neurons to axonal transport defects induced by mutant huntingtin. J. Neurosci. 2008; 28:13662–13672. [PubMed: 19074039]

Herkenham M, Lynn AB, Johnson MR, Melvin LS, de Costa BR, Rice KC. Characterization and localization of cannabinoid receptors in rat brain: a quantitative *in vitro* autoradiographic study. J. Neurosci. 1991; 11:563–583. [PubMed: 1992016]

Hohmann AG, Herkenham M. Localization of cannabinoid CB (1) receptor mRNA in neuronal subpopulations of rat striatum: a double-label *in situ* hybridization study. Synapse. 2000; 37:71–80. [PubMed: 10842353]

Hudson BD, Hebert TE, Kelly ME. Physical and functional interaction between CB1 cannabinoid receptors and beta2-adrenoceptors. Br. J. Pharmacol. 2010; 160:627–642. [PubMed: 20590567]

Ibanez-Sandoval O, Tecuapetla F, Unal B, Shah F, Koos T, Tepper JM. A novel functionally distinct subtype of striatal neuropeptide Y interneuron. J. Neurosci. 2011; 31:16757–16769. [PubMed: 22090502]

Isokawa M. Time-dependent induction of CREB phosphorylation in the hippocampus by the endogenous cannabinoid. Neurosci. Lett. 2009; 457:53–57. [PubMed: 19429161]

Johnson MA, Rajan V, Miller CE, Wightman RM. Dopamine release is severely compromised in the R6/2 mouse model of Huntington's disease. J. Neurochem. 2006; 97:737–746. [PubMed: 16573654]

Kofalvi A, Rodrigues RJ, Ledent C, Mackie K, Vizi ES, Cunha RA, Sperlagh B. Involvement of cannabinoid receptors in the regulation of neurotransmitter release in the rodent striatum: a combined immunochemical and pharmacological analysis. J. Neurosci. 2005; 25:2874–2884. [PubMed: 15772347]

Kreitzer AC. Physiology and pharmacology of striatal neurons. Annu. Rev. Neurosci. 2009; 32:127–147. [PubMed: 19400717]

Kreitzer AC, Malenka RC. Dopamine modulation of state-dependent endocannabinoid release and long-term depression in the striatum. J. Neurosci. 2005; 25:10537–10545. [PubMed: 16280591]

Lee WC, Yoshihara M, Littleton JT. Cytoplasmic aggregates trap polyglutamine-containing proteins and block axonal transport in a Drosophila model of Huntington's disease. Proc. Natl. Acad. Sci. USA. 2004; 101:3224–3229. [PubMed: 14978262]

Li H, Li SH, Cheng AL, Mangiarini L, Bates GP, Li XJ. Ultrastructural localization and progressive formation of neuropil aggregates in Huntington's disease transgenic mice. Hum. Mol. Genet. 1999; 8:1227–1236. [PubMed: 10369868]

Lin CH, Tallaksen-Greene S, Chien WM, Cearley JA, Jackson WS, Crouse AB, Ren S, Li XJ, Albin RL, Detloff PJ. Neurological abnormalities in a knock-in mouse model of Huntington's disease. Hum. Mol. Genet. 2001; 10:137–144. [PubMed: 11152661]

Luthi-Carter R, Strand A, Peters NL, Solano SM, Hollingsworth ZR, Menon AS, Frey AS, Spektor BS, Penney EB, Schilling G, Ross CA, Borchelt DR, Tapscott SJ, Young AB, Cha JH, Olson JM. Decreased expression of striatal signaling genes in a mouse model of Huntington's disease. Hum. Mol. Genet. 2000; 9:1259–1271. [PubMed: 10814708]

Mangiarini L, Sathasivam K, Seller M, Cozens B, Harper A, Hethe-rington C, Lawton M, Trottier Y, Lehrach H, Davies SW, Bates GP. Exon 1 of the HD gene with an expanded CAG repeat is sufficient to cause a progressive neurological phenotype in transgenic mice. Cell. 1996; 87:493–506. [PubMed: 8898202]

Mantamadiotis T, Lemberger T, Bleckmann SC, Kern H, Kretz O, Martin Villalba A, Tronche F, Kellendonk C, Gau D, Kapfhammer J, Otto C, Schmid W, Schutz G. Disruption of CREB function in brain leads to neurodegeneration. Nat. Genet. 2002; 31:47–54. [PubMed: 11967539]

Marsicano G, Wotjak CT, Azad SC, Bisogno T, Rammes G, Cascio MG, Hermann H, Tang J, Hofmann C, Zieglgansberger W, Di Marzo V, Lutz B. The endogenous cannabinoid system controls extinction of aversive memories. Nature. 2002; 418:530–534. [PubMed: 12152079]

Marsicano G, Goodenough S, Monory K, Hermann H, Eder M, Cannich A, Azad SC, Cascio MG, Gutierrez SO, van der Stelt M, Lopez-Rodriguez ML, Casanova E, Schutz G, Zieglgansberger W,

Di Marzo V, Behl C, Lutz B. CB1 cannabinoid receptors and on-demand defense against excitotoxicity. Science. 2003; 302:84–88. [PubMed: 14526074]

Massouh M, Wallman MJ, Pourcher E, Parent A. The fate of the large striatal interneurons expressing calretinin in Huntington's disease. Neurosci. Res. 2008; 62:216–224. [PubMed: 18801393]

Matyas F, Yanovsky Y, Mackie K, Kelsch W, Misgeld U, Freund TF. Subcellular localization of type 1 cannabinoid receptors in the rat basal ganglia. Neuroscience. 2006; 137:337–361. [PubMed: 16289348]

McCaw EA, Hu H, Gomez GT, Hebb AL, Kelly ME, Denovan-Wright EM. Structure, expression and regulation of the cannabinoid receptor gene (CB1) in Huntington's disease transgenic mice. Eur. J. Biochem. 2004; 271:4909–4920. [PubMed: 15606779]

Miller BR, Bezprozvanny I. Corticostriatal circuit dysfunction in Huntington's disease: intersection of glutamate, dopamine and calcium. Future Neurol. 2010; 5:735–756. [PubMed: 21977007]

Miller J, Arrasate M, Brooks E, Libeu CP, Legleiter J, Hatters D, Curtis J, Cheung K, Krishnan P, Mitra S, Widjaja K, Shaby BA, Lotz GP, Newhouse Y, Mitchell EJ, Osmand A, Gray M, Thulasiramin V, Saudou F, Segal M, Yang XW, Masliah E, Thompson LM, Muchowski PJ, Weisgraber KH, Finkbeiner S. Identifying polyglutamine protein species *in situ* that best predict neurodegeneration. Nat. Chem. Biol. 2011; 7:925–934. [PubMed: 22037470]

Milnerwood AJ, Gladding CM, Pouladi MA, Kaufman AM, Hines RM, Boyd JD, Ko RW, Vasuta OC, Graham RK, Hayden MR, Murphy TH, Raymond LA. Early increase in extrasynaptic NMDA receptor signaling and expression contributes to phenotype onset in Huntington's disease mice. Neuron. 2010; 65:178–190. [PubMed: 20152125]

Narushima M, Uchigashima M, Hashimoto K, Watanabe M, Kano M. Depolarization-induced suppression of inhibition mediated by endocannabinoids at synapses from fast-spiking interneurons to medium spiny neurons in the striatum. Eur. J. Neurosci. 2006; 24:2246–2252. [PubMed: 17042791]

Okamoto S, Pouladi MA, Talantova M, Yao D, Xia P, Ehrnhoefer DE, Zaidi R, Clemente A, Kaul M, Graham RK, Zhang D, Vincent Chen HS, Tong G, Hayden MR, Lipton SA. Balance between synaptic versus extrasynaptic NMDA receptor activity influences inclusions and neurotoxicity of mutant huntingtin. Nat. Med. 2009; 15:1407–1413. [PubMed: 19915593]

Palop JJ, Chin J, Mucke L. A network dysfunction perspective on neurodegenerative diseases. Nature. 2006; 443:768–773. [PubMed: 17051202]

Richfield EK, Herkenham M. Selective vulnerability in Huntington's disease: preferential loss of cannabinoid receptors in lateral globus pallidus. Ann. Neurol. 1994; 36:577–584. [PubMed: 7944290]

Rosas HD, Koroshetz WJ, Chen YI, Skeuse C, Vangel M, Cudkowicz ME, Caplan K, Marek K, Seidman LJ, Makris N, Jenkins BG, Goldstein JM. Evidence for more widespread cerebral pathology in early HD: an MRI-based morphometric analysis. Neurology. 2003; 60:1615–1620. [PubMed: 12771251]

Rubino T, Vigano D, Premoli F, Castiglioni C, Bianchessi S, Zippel R, Parolaro D. Changes in the expression of G protein-coupled receptor kinases and beta-arrestins in mouse brain during cannabinoid tolerance: a role for RAS-ERK cascade. Mol. Neurobiol. 2006; 33:199–213. [PubMed: 16954596]

Silva AJ, Kogan JH, Frankland PW, Kida S. CREB and memory. Annu. Rev. Neurosci. 1998; 21:127–148. [PubMed: 9530494]

Stella N, Piomelli D. Receptor-dependent formation of endogenous cannabinoids in cortical neurons. Eur. J. Pharmacol. 2001; 425:189–196. [PubMed: 11513837]

Tepper JM, Tecuapetla F, Koos T, Ibanez-Sandoval O. Heterogeneity and diversity of striatal GABAergic interneurons. Front. Neuroanat. 2010; 4:150. [PubMed: 21228905]

Uchigashima M, Narushima M, Fukaya M, Katona I, Kano M, Watanabe M. Subcellular arrangement of molecules for 2-arachidonoyl-glycerol-mediated retrograde signaling and its physiological contribution to synaptic modulation in the striatum. J. Neurosci. 2007; 27:3663–3676. [PubMed: 17409230]

Van Laere K, Casteels C, Dhollander I, Goffin K, Grachev I, Bormans G, Vandenberghe W. Widespread decrease of type 1 cannabinoid receptor availability in Huntington disease *in vivo*. J. Nucl. Med. 2010; 51:1413–1417. [PubMed: 20720046]

Vonsattel JP, Myers RH, Stevens TJ, Ferrante RJ, Bird ED, Richardson EP Jr. Neuropathological classification of Huntington's disease. J. Neuropathol. Exp. Neurol. 1985; 44:559–577. [PubMed: 2932539]

Walker FO. Huntington's disease. Lancet. 2007; 369:218–228. [PubMed: 17240289]

Woodman B, Butler R, Landles C, Lupton MK, Tse J, Hockly E, Moffitt H, Sathasivam K, Bates GP. The Hdh(Q150/Q150) knock-in mouse model of HD and the R6/2 exon 1 model develop comparable and widespread molecular phenotypes. Brain Res. Bull. 2007; 72:83–97. [PubMed: 17352931]
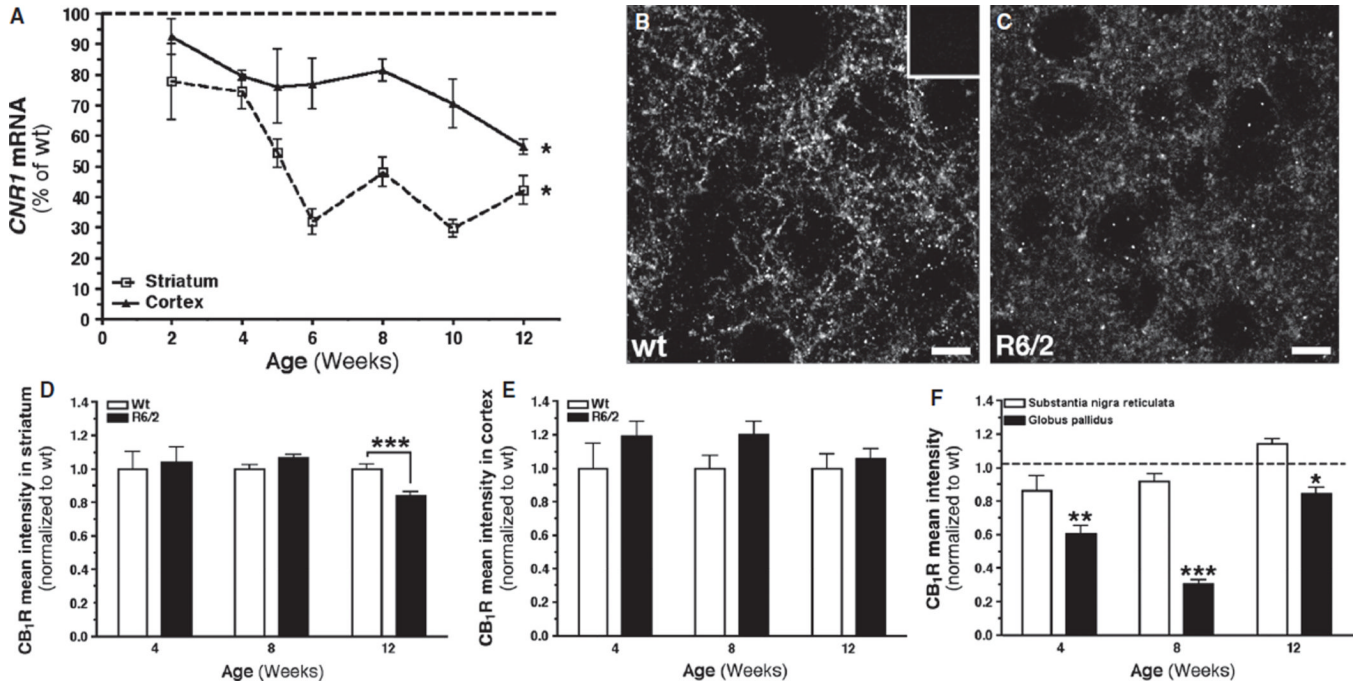
Fig. 1.
Expression of total CB_1 receptor in the sensorimotor cortex and basal ganglia of R6/2 mice. (A) qPCR time course of *CNR1* mRNA in the cortex and striatum of R6/2 mice normalized to percentage of levels measured in wild-type littermates ($n = 3$–5 mice; Str R6/2 vs. WT genotype: df = 1, $F = 72.495$, $*P < 0.05$; Ctx R6/2 vs. WT genotype: df = 1, $F = 18.839$, $*P < 0.05$; Str and Ctx R6/2 vs. WT age: ns, two-way ANOVA). (B and C) Representative CB_1 receptor labeling in the striatum of 12-week-old wild-type mice displaying characteristic axonal labeling that is decreased in 12-week-old R6/2 littermates (insert: CB_1 receptor labeling in $CB_1^{-/-}$ scale bar: 20 mm). (D) Time course of total CB_1 receptor expression quantified by sq-IHC in the striatum of R6/2 compared with wild-type littermates [$n = 4$ mice (4 weeks), 5 mice (8 weeks), 4–5 mice (12 weeks); $***P < 0.001$]. (E) Time course of total CB_1 receptor in the sensorimotor cortex of 12-week-old R6/2 and wild-type littermates [$n = 4$ mice (4 weeks), 5 mice (8 weeks), 4–5 mice (12 weeks)]. (F) Time course of CB_1 receptor expression in the globus pallidus and substantia nigra pars reticulata of R6/2 mice quantitated by sq-IHC ($n = 3$ mice per age and genotype, $*P < 0.05$, $**P < 0.01$, $***P < 0.001$). All sq-IHC values are expressed as mean ± SEM normalized to age-matched wild-type CB_1 receptor expression, and analysed by two-tailed Student's *t*-test to their wild-type littermates.
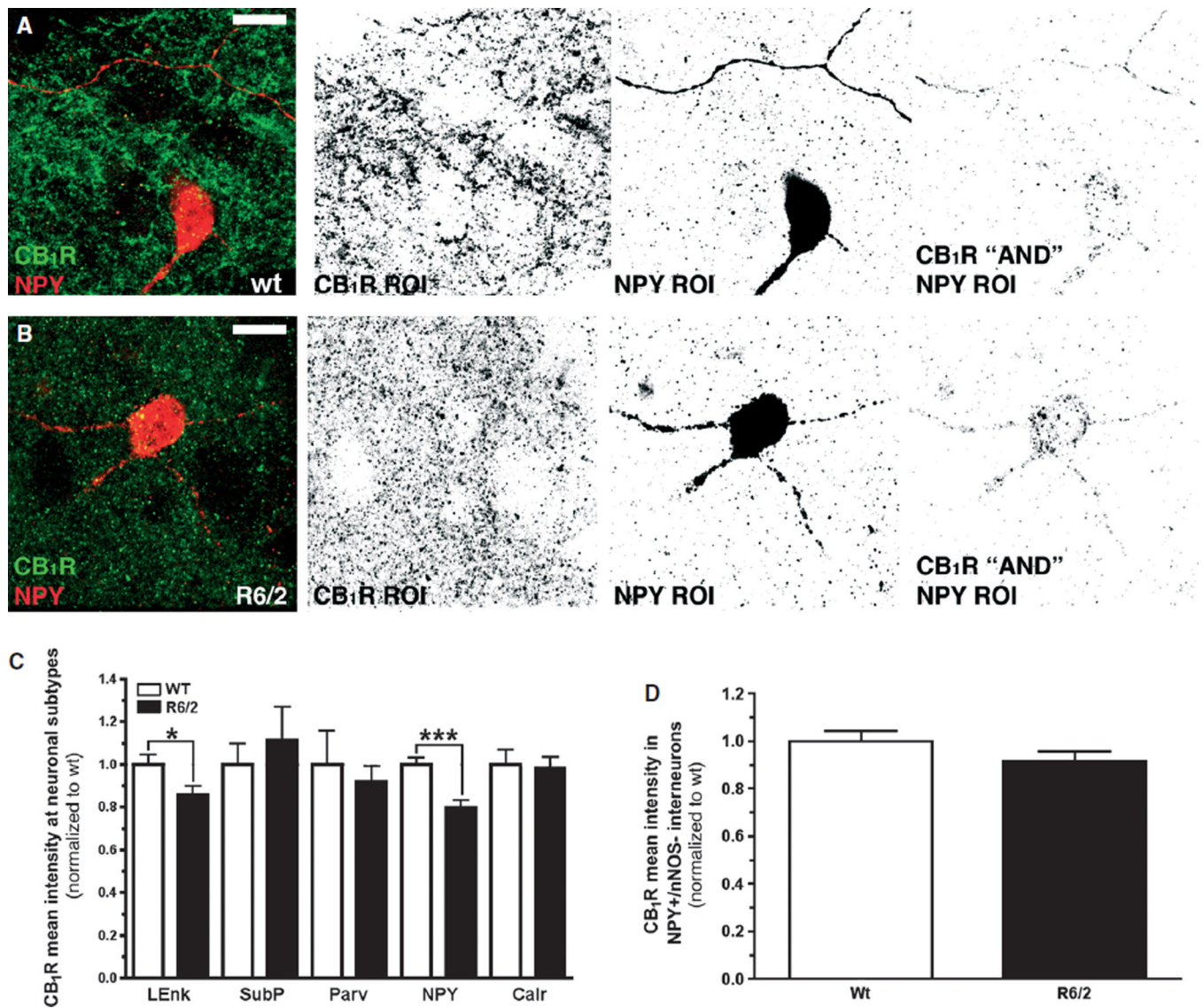
Fig. 2.
sq-IHC analysis of CB_1 receptor at neuronal subtypes and synapses in the striatum of 12-week-old R6/2 mice. (A and B) Representative dual-labeled images of CB_1 receptor (Lin *et al.*, 2001) and neuropeptide Y (NPY; Blazquez *et al.*, 2011) interneurons in the striatum and the regions of interest (ROIs; see Materials and methods) created to identify positive CB_1 receptor pixels (CB_1 ROI), NPY pixels (NPY ROI), and overlapping CB_1 receptor and NPY pixels [(CB_1 'AND' NPY ROI); scale bar: 20 mm]. (C) CB_1 receptor expression at indirect pathway [leucine-enkephalin (LEnk)] and direct pathway [substance P (SubP)] axonal collaterals, parvalbumin (Parv) and NPY interneurons in the striatum of wild-type and R6/2 mice ($n = 4$–5 mice, $*P < 0.05$, $***P < 0.001$). (D) CB_1 receptor expression at NPY/neuronal nitric oxide synthase (nNOS—) interneurons in the striatum of wild-type and R6/2 mice ($n = 5$ mice). All values are expressed as mean ± SEM normalized to age-matched wild-type CB_1 receptor expression, and analysed by two-tailed Student's *t*-test to their wild-type littermates.
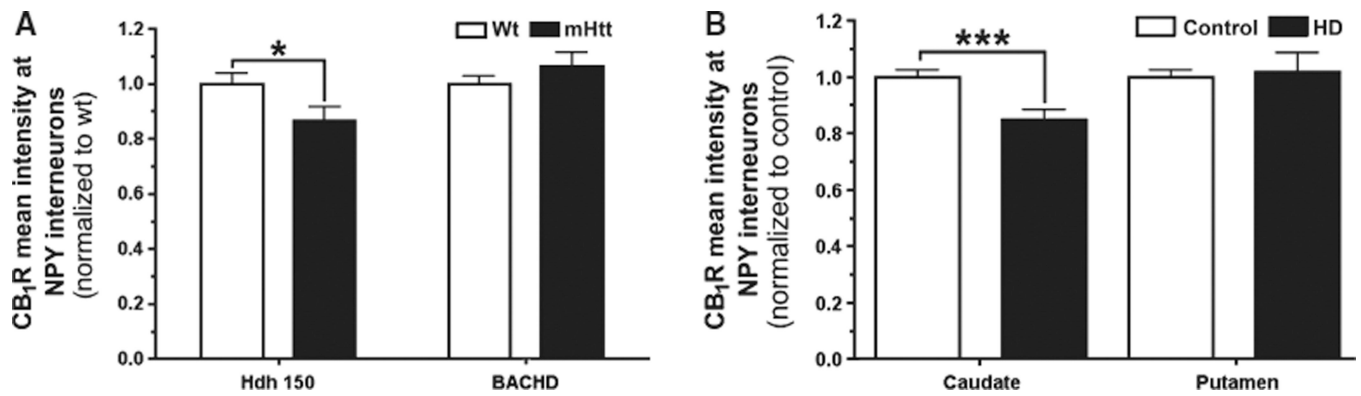
Fig. 3.
CB_1 receptor expression at neuropeptide Y (NPY) interneurons in full-length HD mouse models and human patients with HD. (A) sq-IHC analysis of striatal sections from wild-type and $Hdh^{Q150/Q150}$ or BACHD mice co-labeled for CB_1 receptor, and neuropeptide Y (NPY) to quantify the expression of CB_1 receptor at NPY interneurons [$n = 3$ mice ($Hdh150^{Q150/Q150}$ group), 3–4 mice (BACHD group); *$P < 0.05$]. (B) CB_1 receptor expression in NPY interneurons of the caudate and putamen of *post mortem* patients with HD compared with non-HD patients (control; $n = 5$ patients per condition, ***$P < 0.001$). All values are expressed as mean ± SEM normalized to age-matched wild-type CB_1 receptor expression, and analysed by two-tailed Student's *t-test* to their wild-type littermates.
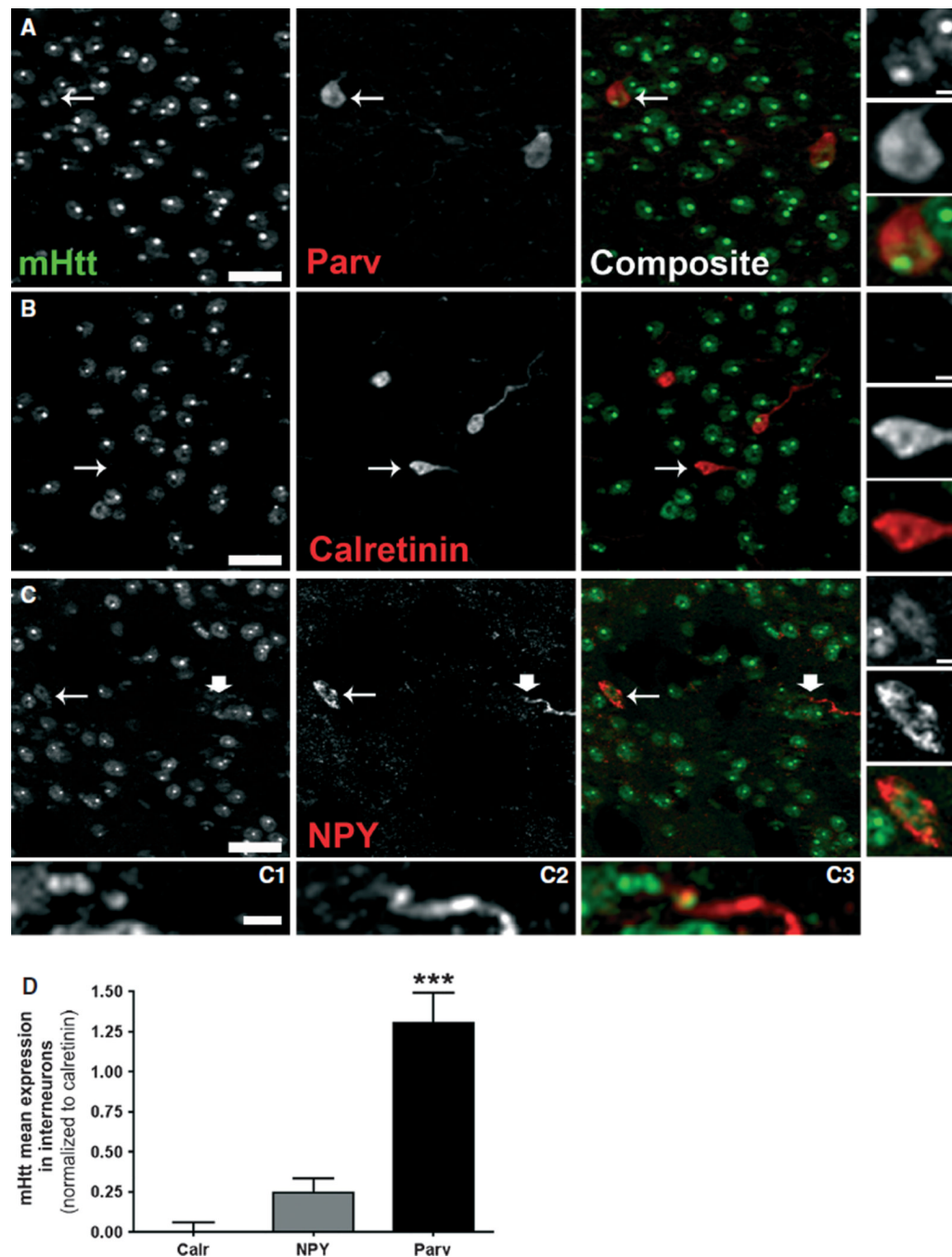
Fig. 4.
Mutant huntingtin (mHtt) expression levels in GABAergic interneurons in the striatum of 12-week-old R6/2 mice. R6/2 striatal tissue sections dual-labeled for mHtt (green, left column; scale bar: 50 μm) and parvalbumin (Parv; A), calretinin (B) or neuropeptide Y (NPY; C) interneurons (red, middle column). Small inserts on the right are magnified images of mHtt expression in the soma of each interneuron subtype as identified by a thin arrow in the parent image (scale bar: 5 μm). (C3) Magnified image of an NPY-labeled neurite (C2) containing a mHtt aggregate (C1, scale bar: 10 μm). (D) sq-IHC analysis of the expression level of mHtt within each subtype of striatal interneuron normalized to calretinin levels expressing levels close to background levels ($n = 5$ R6/2 mice, ***$P < 0.001$

compared with calretinin and NPY subtypes). All values are expressed as mean ± SEM normalized to mHtt mean intensity in calretinin interneurons, and analysed by one-way ANOVA with Tukey's *post hoc* analysis.
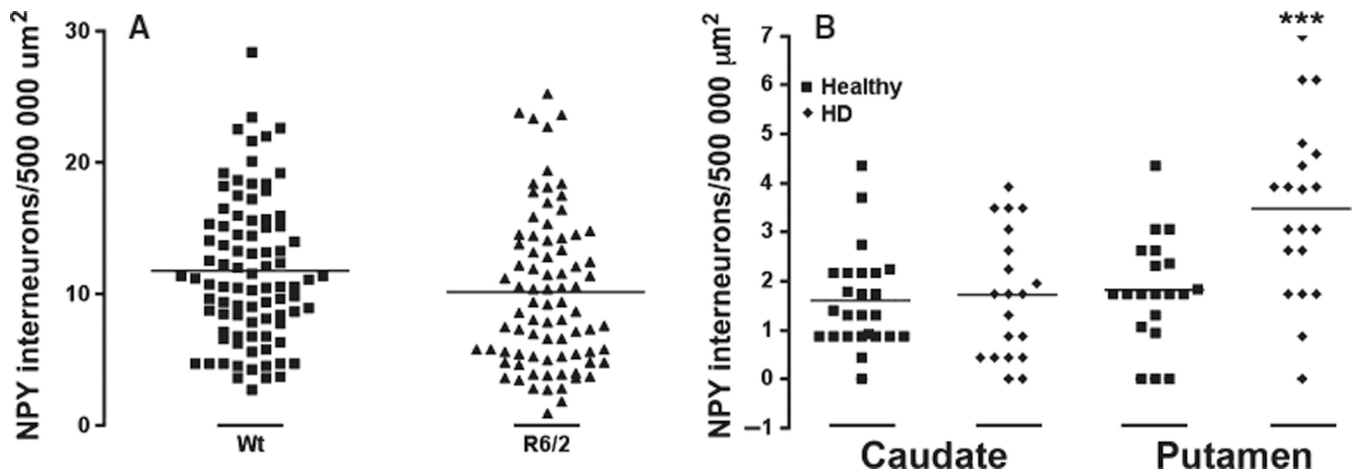
Fig. 5.
Population of neuropeptide Y (NPY) interneurons in the striatum of 12-week-old R6/2 mice and the caudate-putamen of patients with HD. (A) Number of NPY-positive soma in the dorsolateral striatum of 12-week-old R6/2 compared with wild-type littermates ($n = 10$ mice per genotype). (B) NPY-positive neurons in the caudate and putamen of HD and non-HD (control) patients ($n = 5$ per group; ***$P < 0.001$ for patients with HD compared with the population of NPY interneurons in the caudate and putamen of control and caudate of patients with HD). All values are expressed as mean ± SEM per area, and were analysed by a two-tailed Student's *t-test* in (A) a one-way ANOVA, with Tukey's *post hoc* analysis in (B).
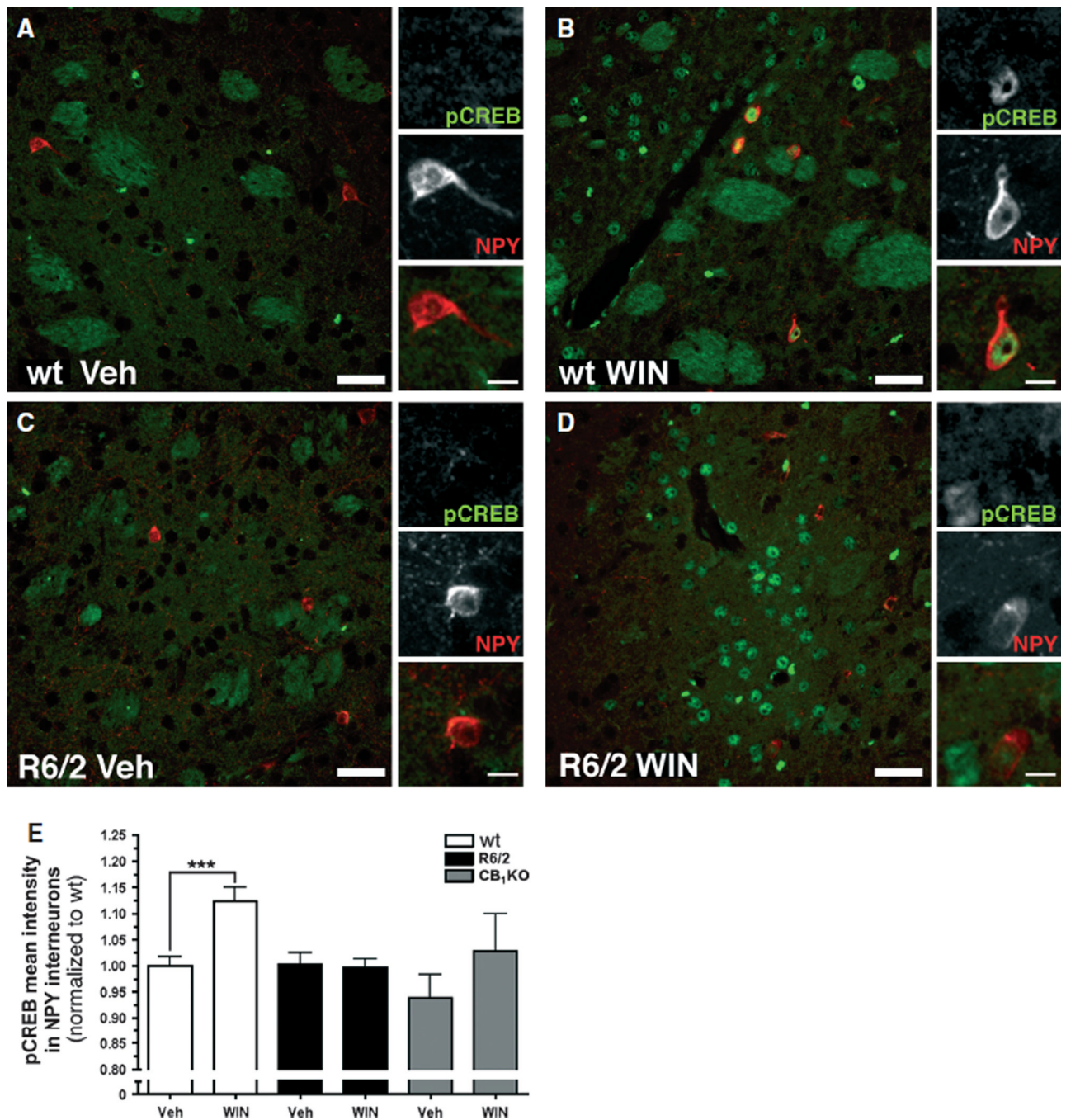
Fig. 6.
Phosphorylated cAMP response element-binding protein (pCREB) in striatal neuropeptide Y (NPY) interneurons following *in vivo* WIN 55,212-2 administration. (A–D) Striatal sections from 12-week-old R6/2 and wild-type littermates dual-labeled for pCREB (green) and NPY (Blazquez *et al.*, 2011) 30 min following i.p. administration of WIN 55,212-2 or vehicle (scale bar: 100 μm). Enlarged images of NPY interneurons depicting the presence or absence of nuclear pCREB staining (left three panels of A–D; scale bar: 10 μm). (E) sq-IHC of pCREB increases in striatal NPY interneurons of 12-week-old R6/2 and wild-type littermates 30 min following treatment with WIN 55,212-2 or vehicle ($n = 5$ mice; ****P<*

0.001). All values are expressed as mean ± SEM normalized to age-matched wild-type pCREB expression, and analysed by a one-way ANOVA with Tukey's *post hoc* test.

Table 1

ROIs created for sq-IHC

ROI	Gating	Measurements
1	Mean + Standard Deviation	CB_1R mean intensity
2	Mean + Standard Deviation	Neuronal subtype mean intensity
3	ROI 1 "AND" ROI 2	CB_1R expression at neuronal subtype